LAMINAR FLOW NUMERICAL STUDY USING FINITE ELEMENTS METHOD AND CHARACTERISTIC-BASED SPLIT ALGORITHM FOR A SAME PRESSURE AND VELOCITY INTERPOLATION ORDER

Rafael de Mello Pereira
Campos Darci Ribeiro – Universidade de Brasília – Departamento de Engenharia Mecânica – Laboratório de Energia e Ambiente
CEP 70.910-900 – Brasília – DF – Brasil
+55(61) 307-2314 R236/238
rpereira_01@bol.com.br

Antônio C. P. Brasil Júnior
brasil@enm.unb.br

Abstract. *This work presents a numerical study of laminar flows using the finite element method with the characteristic-based split stabilization technique. The used algorithm avoids the use of different meshes for pressure and velocity, allowing a same interpolation order for both. The algorithm is presented in its semi-implicit version which demands the solution of only one system of equation per iteration. Classical geometries like the lid-driven cavity for two and three dimension and the backward-facing step are used for evaluate the algorithm performance. The obtained results are compared with a wide numerical bibliography and, when available, with experimental works.*

Keywords*: finite elements, characteristic-based split, laminar flow*

1. Introduction

The finite element method has been used with increasing success during the last three decades on fluid flow simulations. Even though, other techniques like finite volumes were previously employed in flow simulation, and keep being the most used tool for this research area, the finite element method has achieved maturity along the last years. The advances in stabilization techniques contributed for the use of the method in strongly non-linear equations like the ones which are necessary to describe a fluid continuous media. In the present work a stabilization technique named Characteristic-Based Split with triangular linear elements will be studied and assessed using classical laminar flow cases.

For laminar flow simulation the employed set of equations are the Navier-Stokes equations themselves avoiding any average process and turbulence modeling. The Reynolds number used shall also be kept low. In spite of the apparent simplicity the adequate solution to this problem is essential for the solution to more sophisticated cases where, for example, a turbulence model is used or the fluid has a Non-Newtonian behavior. Furthermore, the responsibility for the convection-diffusion problem stabilization and the LBB restriction accordance are fully present in the laminar case problem, therefore the efficient solution to this case represents a great step in the solutions to more sophisticated problems.

For the finite element method stabilization the Characteristic-Based Split methodology is used. This methodology works in a three step semi-implicit way. The first step of the method demands the solution of an explicit convection-diffusion problem for the velocity field, the second step solve the pressure field implicitly and the last one corrects the first step velocity using the new pressure field. Using the CBS methodology the pressure and velocity values can be evaluated together in same mesh nodes, avoiding the use of two intercalated meshes. It represents a great numerical advantage considering the simplification it brings to the problem. Other possible simplification allowed by CBS algorithm concern the solution of the linear system of equations in step number two, for this step the conjugated gradient method was choused because the system of equations is symmetric and positive defined.

The code validation is carried out using three classical cases, the bidimensional lid-driven cavity, the backward-facing step and the tri-dimensional lid-driven cavity. The first two cases have been widely employed since the beginning of computer fluid dynamics presenting therefore a good challenger for CFD codes validation. The bibliography is also full of numerical results for these cases. The last case represents a major challenger due its tri-dimensional nature, for this case the results are only compared qualitatively with experimental data.

2. Methodology

The flow is modelled by the incompressible Navier-Stokes equations, written using indicial notation in a Cartesian co-ordinate system as Eq. (1).

$$\rho\left(\frac{\partial u_t}{\partial t}+\frac{\partial}{\partial x_j}\left(u_j u_i\right)\right)=\frac{\partial \tau_{ij}}{\partial x_j}-\frac{\partial p}{\partial x_i}+\rho g_i \tag{1}$$

Where,

$$\tau_{ij} = \mu\left(\frac{\partial u_i}{\partial x_j} + \frac{\partial u_j}{\partial x_i}\right) \tag{2}$$

For an incompressible flow, Eq. (3) shows the continuity equation.

$$\frac{\partial u_i}{\partial x_i} = 0 \tag{3}$$

The governing equations are solved by a finite element method using equal order interpolation for velocity and pressure and linear triangle elements. In this methodology the continuity and momentum equations are solved using a splitting strategy, considering an incremental time integration algorithm with multiple steps. This approach has a stable behaviour depending of the time step used in the incremental time integration.

The aim of the CBS algorithm involves two major ideas (Zienkiewicz, 2000 and Codina, 1998). Firstly the momentum equation is re-written along a characteristic path, in order to reduce the spurious effects due the galerkin discretization for high Reynolds Number. This allows an additional stabilized term in the formulation on streamline direction, equivalent to the streamline-diffusion terms. The second feature of this algorithm is to decouple the pressure and velocity fields through the use of a fractional step algorithm, like in classical splinting-projection schemes (Chorin, 1968 and Teman, 1969). It is shown that this last approach allows a stabilization term for the pressure and velocity discretization spaces (Codina 2001). Those two ingredients of the CBS method permit a stable scheme for convective-advective treatment and for pressure-velocity discretization. The stabilization parameter now is the time step. It can be shown that this scheme has equivalent stabilized properties of other methodologies (Codina 2002). Given the set of variables known in a previous time step t, $(u^{n+}.p^{n+})$. The solution $(u^{n+1}.p^{n+1})$ of the conservation equations in a time step $t+\Delta t$, is obtained following these steps:

Step 1: Solving the time discretization of the momentum equation without the pressure term.

$$\Delta u_i^* = u_i^* - u_i^n = \Delta t\left[-\frac{\partial}{\partial x_j}\left(u_j u_i\right) + \frac{1}{\rho}\frac{\partial \tau_{ij}}{\partial x_j} - g_i + \frac{\Delta t}{2}u_k\frac{\partial}{\partial x_k}\left(\frac{\partial}{\partial x_j}\left(u_j u_i\right) + \rho g_i\right)\right]^n \tag{4}$$

Step 2: Solving the pressure field.

$$\rho\Delta t\theta_1\theta_2\frac{\partial^2 \Delta p}{\partial x_i \partial x_i} = \frac{\partial u_i^n}{\partial x_i} + \theta_1\frac{\partial \Delta u_i^*}{\partial x_i} - \rho\Delta t\theta_1\left(\frac{\partial^2 p^n}{\partial x_i \partial x_i}\right) \tag{5}$$

Where θ_1 and θ_2 are constants equal to 0.5.

Step 3: Solving the Velocity correction – Divergence-free Projection

$$\Delta u_i = u_i^{n+1} - u_i^n = \Delta u_i^* - \Delta t\frac{1}{\rho}\frac{\partial p^{n+\theta_2}}{\partial x_i} - \frac{1}{\rho}\frac{\Delta t^2}{2}u_k\frac{\partial Q_i^n}{\partial x_k} \tag{6}$$

Using the Galerkin method for spatial discretization of the equations on the steps 2-3, coupled to the classical finite element base function, a matrix form of the algorithm can be written as a set of three symmetrical linear systems for each time step.

$$\begin{cases} \mathbf{M}.\Delta\mathbf{u}^* = \mathbf{f}_u^* \\ \mathbf{H}.\mathbf{p} = \mathbf{f}_p \\ \mathbf{M}.\Delta\mathbf{u} = \mathbf{f}_u \end{cases} \tag{7}$$

In those equations $\mathbf{M}$ and $\mathbf{H}$ are the mass and discrete Laplacian matrices given by:

$$\mathbf{M}_{ij} = \int_{\Omega} \mathbf{N}_i \mathbf{N}_j d\Omega \tag{8}$$

$$\mathbf{H}_{ij} = \int \nabla \mathbf{N}_i \nabla \mathbf{N}_j d\Omega \tag{9}$$

The vectors $\mathbf{f}_u^*$, $\mathbf{f}_p$ and $\mathbf{f}_u$ are related to the discretization of the right hand side of the equations on the steps 1-3. The boundary terms, associated to the outflow and inflow conditions, are added into these vectors.

Remarks

The solution of the linear systems at steps 1 and 3 involve the mass matrix. In order to enhance the convergence rate of the computations, this matrix is lumped in a diagonal form. It is performed once in the beginning of the iterative computation.

The linear system for the pressure correction problem, step2, is solved by the Conjugated Gradient Method, preconditioning by partial Cholesky factorization. This matrix is stored by a space Morse strategy, and the preconditioning is also performed once when this matrix is firstly computed.

In the present paper the time step is controlled by the following expressions:

$$\Delta t \leq \frac{\Delta t_c \Delta t_d}{\Delta t_c + \Delta t_d} \tag{10}$$

Where

$$\Delta t_c = \left(2 \left\| \mathbf{u}.\nabla N_i \right\|_{\max}\right)^{-1} \tag{11}$$

and

$$\Delta t_c = \left(2\mu^e \left\| \nabla N_i . \nabla N_j \right\|_{\max}\right)^{-1} \tag{12}$$

These expressions consider the characteristic times for the diffusion and convection counterpart of the discrete problem, at each element. It can be verified that the critical time step proposed by the Eqs. (10-12) follows the relation:

$$\Delta t \leq \left(c_1 \frac{\mu^e}{h^2} + c_2 \frac{\left|\mathbf{u}^n\right|}{h} \right)^{-1} \tag{13}$$

Where c_1 and c_2 are constants and h denotes a characteristic length of the element. It can assure the stability of the scheme following the analysis of (Codina 2002) for instance.

3. Results

In this section three numerical examples are presented in order to validate the laminar code. These cases are classical benchmark cases which have been studied for years.

3.1. Cavity

The first case used to assess the code is the classical lid-driven cavity flow. This case was firstly employed for code validation by (Ghia et. Al., 1982) and since then has been used by many researcher as a reference. Figure 1 shows the utilized geometry and boundary conditions. The problem has a square domain with the top side driving with a unitary speed, the other sides are walls. A pressure constrainement is also applied in the middle of the bottom wall. A structured mesh with 1681 nodes is employed with a geometric refinement progression of 0.1 to assure a finer mesh near the walls. This case was simulated using four different Reynolds number, 100, 400, 1000 and 5000.

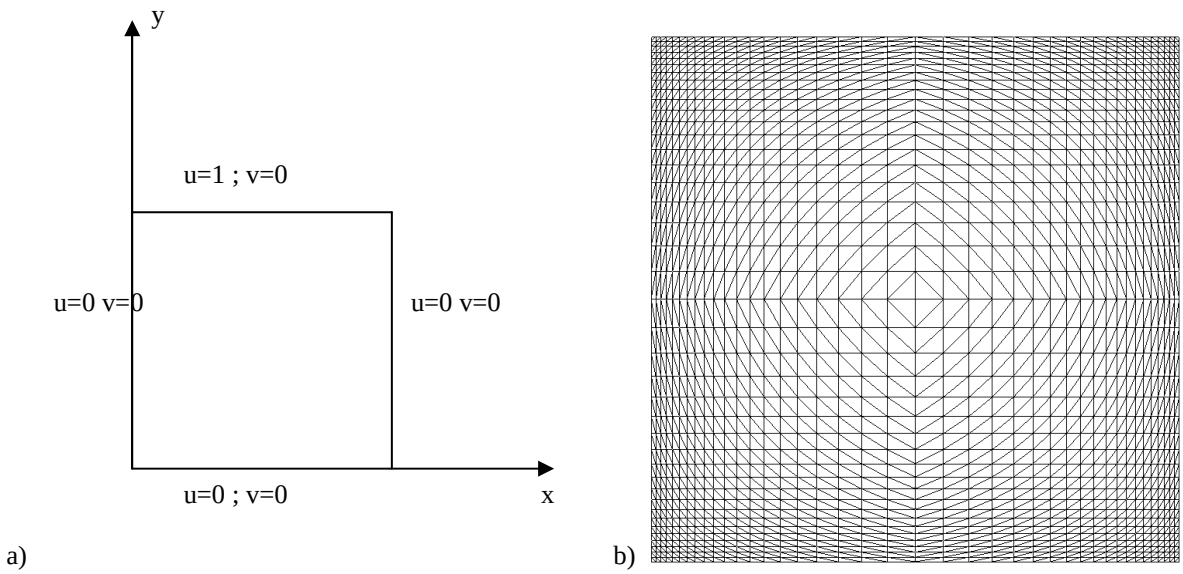

Figure 1. Geometry, boundary conditions and used mesh.

A vertical and horizontal velocity profile in the mid of the cavity is shown in Figure 3. The results are ploted together with (Ghia et Al, 1982) results. It is remarkable how both results fit well even though the Ghia compared results were obtained using finite differences and a much finer mesh with 129 X 129 lateral divisions. The pressure and velocity profile agreed also with the results obtained by (Macedo 1995) and (Akin 1994) using the finite element method.

Figure 2a shows the stream lines for the highest Reynolds Number, it is possible to see that the velocity field is well developed in the entire domain without any oscillation. The singularity point behaviour shown by Figure (2b) was observed by other researcher using finer meshes.

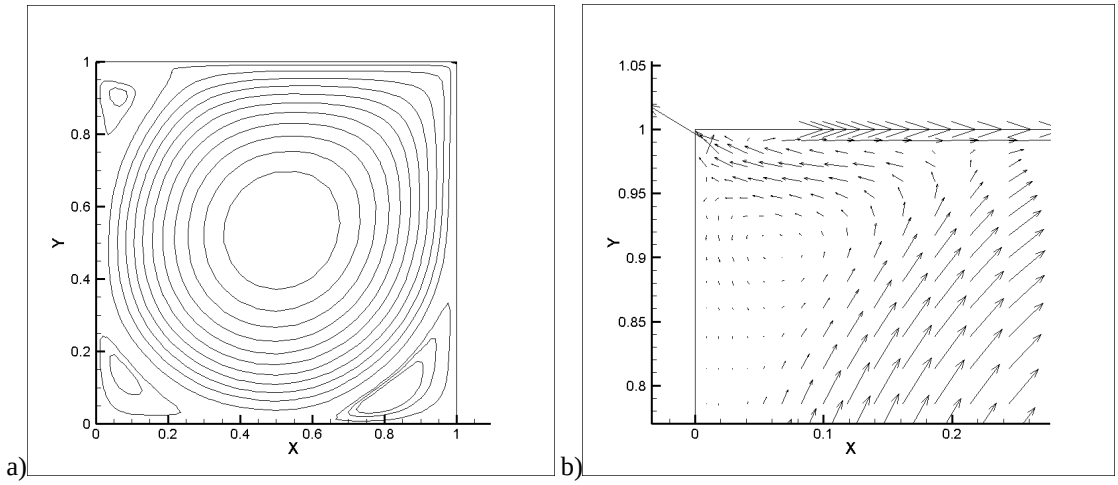

Figure 2. Velocity field: Re=5000, a) Stream lines, b) Upper left corner vortex detail.

3.2. Backward-faced step

Many usual engineering applications have recirculation zones. To test and validate CFD codes over these recirculation conditions the backward-facing step case has been used for years. Figure 4 shows the geometries used. The boundary conditions adopted are an inlet parabolic *u* velocity profile together with a zero vertical velocity *v* Non-slip conditions are enforced on all solid walls. For out-flow a Neumann condition is imposed with a zero pressure restriction. Two different geometries are used:

- Geometry 1: H=1.5, h=1.0, L=22 and l=3
- Geometry 2: H=1,0, h=0.5, L=22 and l=3

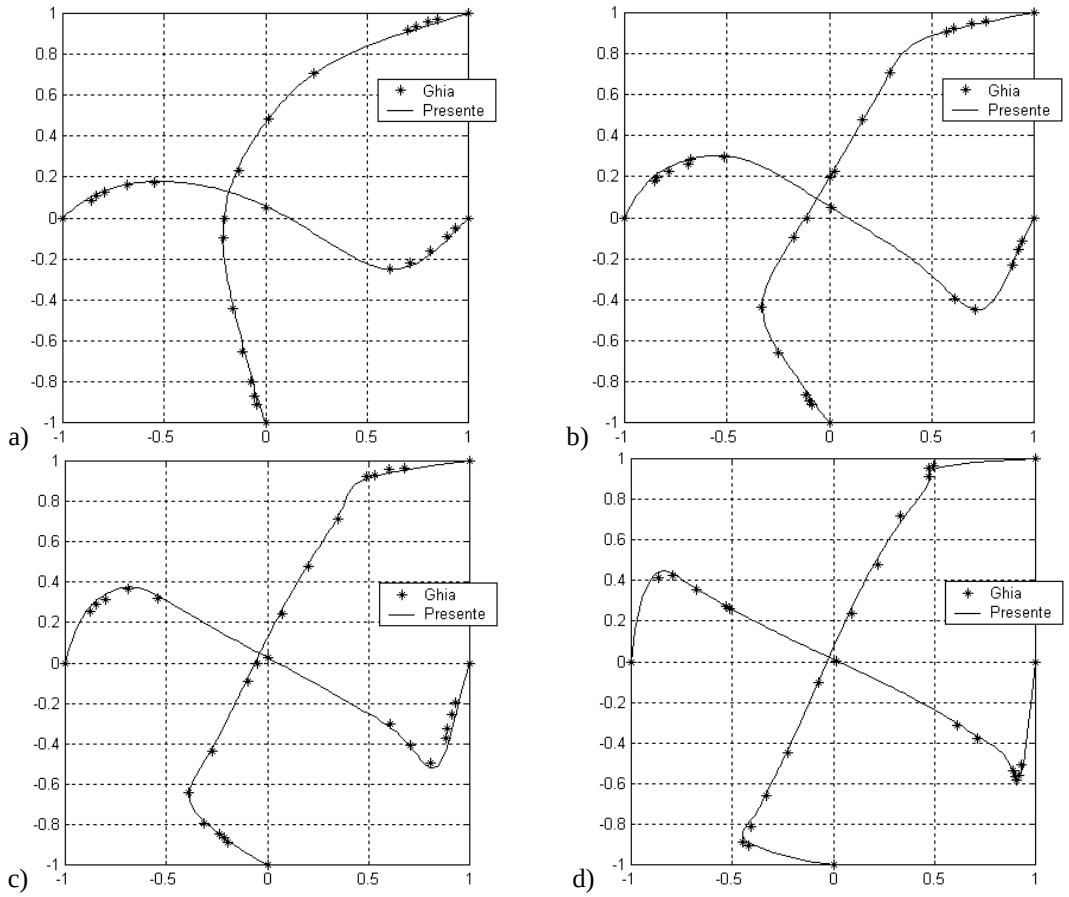

Figure 3. Velocity profile for a horizontal and vertical mid line. a)Re=100, b)Re=400, c)Re=1000, d)Re=5000

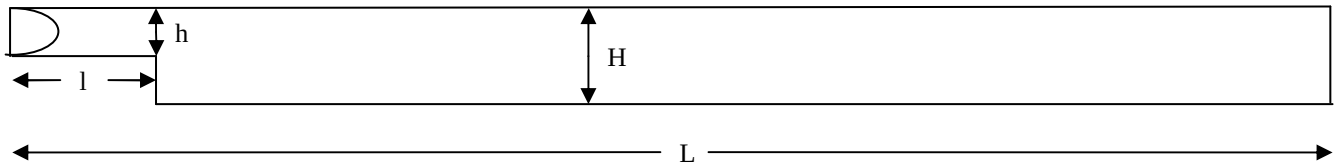

Figure 4. Used Geometry for the Backward-Faced step.

Altogether four cases were simulated with two Reynolds number Re=50 and Re=150 being used for each geometry

i) Geometry (1), Re=50, mesh with 2017 nodes and 3840 elements.
ii) Geometry (2), Re=50, mesh with 2017 nodes and 3840 elements.
iii) Geometry (1), Re=150, mesh with 2017 nodes and 3840 elements.
iv) Geometry (2), Re=150, mesh with 2017 nodes and 3840 elements.

Reynolds number is defined by:

$$\mathrm{Re} = \frac{|\mathbf{u}|_{\max}(H-h)}{\nu} \tag{14}$$

The results obtained show that the velocity is well developed over the entire domain. The big recirculation zone at the step bottom, that is the main characteristic of this problem, is also present. The predicted results agree quite well with the results obtained for many researchers (Morgan, K., Periaux, J., Thomasset, F., 1982). A comparison with some of these results shows a suitable agreement for the vortex reattachment point and the maximum and minimum velocity in two different points after the step. Those comparisons are shown in Tables 1,2 and 3 where the distance after the step is calculated by:

$$d = x/(H-h) \tag{15}$$

Table 1. Horizontal velocities, u, d=1.6 (after the step)

Results	Case (i)		Case (ii)		Case (iii)		Case (iv)	
	Min.	Max.	Min.	Max.	Min.	Max.	Min.	Max.
Present study	-0.05	0.91	-0.04	0.71	-0.07	0.97	-0.10	0.90
Kueny-Binder	-0.04	0.90	-	-	-0.07	0.97	-0.09	0.92
Buffat et. al.	-0.05	0.89	-0.02	0.69	-0.07	0.95	-0.11	0.88
Dhatt-Hubert	-0.05	0.86	-0.05	0.74	-0.06	0.96	-0.10	0.91
Donea et. al.	-0.06	0.91	-0.06	0.73	-0.08	0.97	-0.10	0.90
Ecer et. al.	-0.06	0.91	-0.06	0.72	-0.09	0.92	-0.04	0.87
Glowinski et. al.	-0.04	0.91	-0.03	0.71	-0.07	0.96	-0.10	0.90
Hecht	-0.05	0.91	-0.04	0.72	-0.07	0.97	-0.103	0.90

Table 2. Horizontal velocities, u, d=4.0 (after the step)

Results	Case (i)		Case (ii)		Case (iii)		Case (iv)	
	Min.	Max.	Min.	Max.	Min.	Max.	Min.	Max.
Present study	0.00	0.78	0.00	0.52	-0.05	0.91	-0.045	0.72
Kueny-Binder	0.00	0.72	-	-	-0.05	0.93	-0.016	0.71
Buffat et. al.	0.00	0.77	0.00	0.52	-0.05	0.90	-0.03	0.70
Dhatt-Hubert	0.00	0.78	0.00	0.52	-0.03	0.91	-0.04	0.72
Donea et. al.	0.00	0.78	0.00	0.53	-0.06	0.91	-0.06	0.72
Ecer et. al.	0.00	0.77	0.00	0.53	-0.03	0.87	-0.03	0.71
Glowinski et. al.	0.00	0.77	0.00	0.52	-0.05	0.91	-0.05	0.72
Hecht	0.00	0.78	0.00	0.52	-0.05	0.91	-0.05	0.73

Table 3. Reattachment point (after the step).

Results	Case (i)	Case (ii)	Case (iii)	Case (iv)
Present study	3.02	2.1	6.775	4.9
Kueny-Binder	3.0	-	6.0	4.5
Buffat et. al.	2.5	1.0	5.8	4.5
Dhatt-Hubert	3.0	2.0	6.5	5.0
Donea et. al.	2.5	2.0	6.0	5.0
Ecer et. Al.	3.0	2.8	5.9	4.7
Glowinski et. al.	2.5	1.8	5.8	4.4
Hecht	2.76	2.1	6.0	4.6

Figure 5 shows that qualitatively the velocity field is well developed through the domain and the pressure field is free of oscillations Fig 6. Visually these results agree quite well with those obtained by (Macedo 1995).

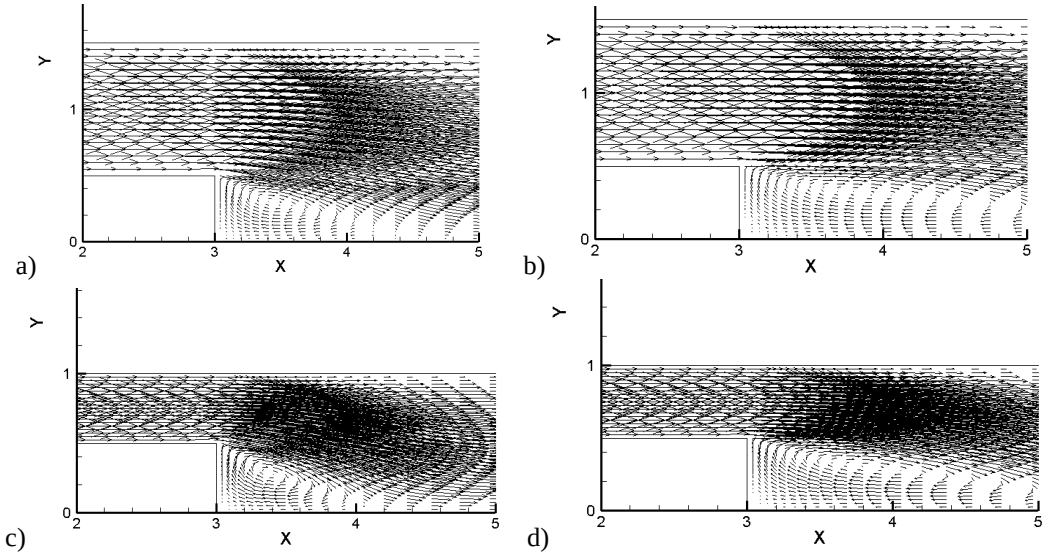

Figura (5) – Velocidade na zona de recirculação do degrau, a) caso (i), b) caso (iii), c) caso (ii) , d) caso (iv)

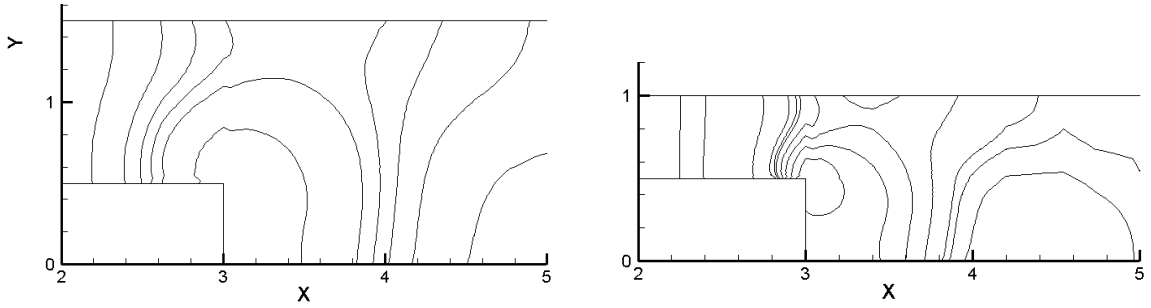

Figura (6) – Pressure field for the step. Case (i) e Case(iii).

3.3. Tri-dimensional lid-driven cavity

The last explored case was the tri-dimensional lid-driven cavity, like the previous bi-dimensional case non-slippery condition is enforced in the walls except the lid which driven with a uniform velocity. In order to simplify the problem it was simulated using a symmetry plane. Figure 7 shows the geometry, boundary condition and the surface of the employed mesh. A common behaviour for this case is the formation of a huge recirculation zone on the midle of the cavity like the bidimensional case but this case shows also the formation of a sequence of vortexes in the XY plane called Taylor-Görtler vortexes (Rhee, 1984). The two kinds of vortexes are also present in the simulation for Re=1000, fig. 9. Figure 8 shows a suitable agreement with the experimental data.

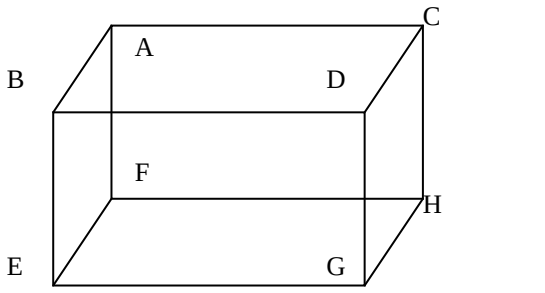

ABEF – Wall ; EFGH – Wall
EGDB – Wall; FHCA – Wall
CDGH – Symmetri plane;ABDC – u=0, v=0, w=1.

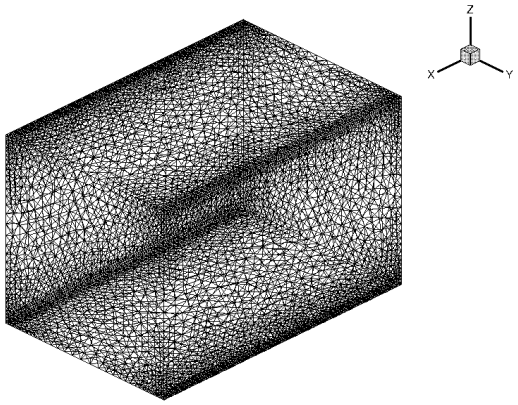

Figura (7) – Cavity 3D: geometry, boundary conditions and surface mesh.

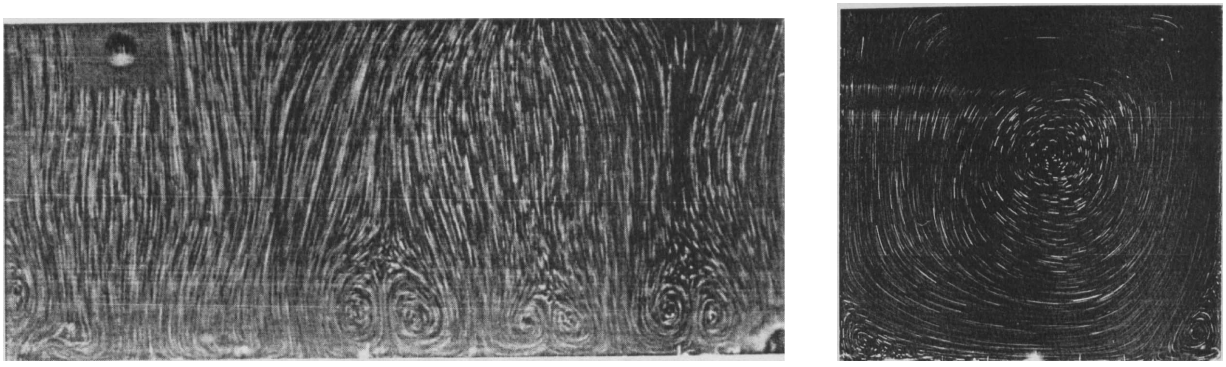

Figure (8) – Cavity 3D: Vortex de Taylor-Görtler and central vortex (experimental).

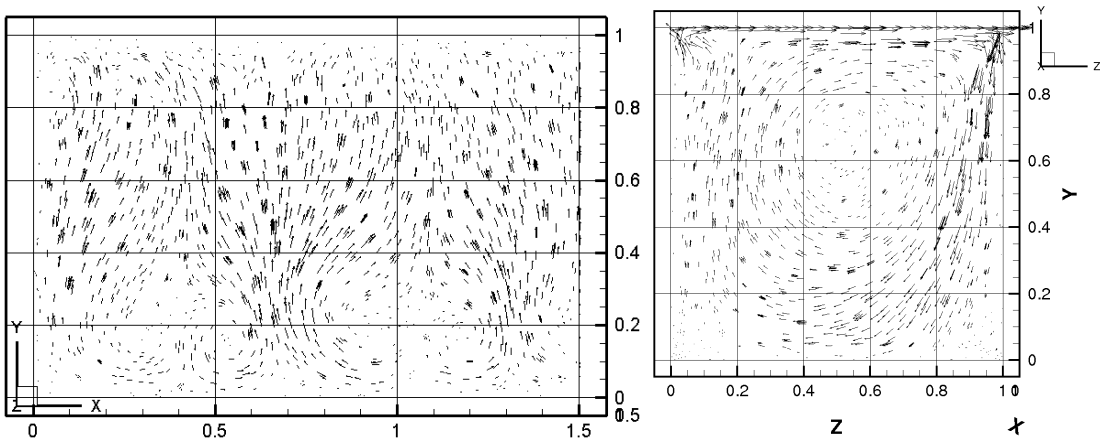

Figure (9) – Cavity 3D: Vortex de Taylor-Görtler and central vortex (numerical).

4. Conclusions

For the three assessed cases the Characteristic-Based split algorithm seems to be very stable for bi and tri-dimensional problems. Concerning the bi-dimensional lid-driven cavity the middle velocity results fit remarkable well with the studied bibliography even when compared with other numerical methods like the finite differences method using finer meshes. The backward-faced step reattachment point results are well inserted in the range found in bibliography, the pressure and velocity fields are continuous and smooth with no oscillation and the maximum and minimum velocities also agree with the bibliography. The tri-dimensional lid-driven cavity problem was more computationally expensive, so it was not possible to use a finer grid and higher Reynolds number, even though it still possible to capture the characteristically behavior of this problem and the results agree quite well quantitatively with the experimental data.

The choose algorithm was easily implemented with the greet advantage of using only one mesh for pressure and velocity it shows that this algorithm circumvent the Babuska-Brezzi restriction. Other noticed numerical advantage was the necessity of solve only one symmetrical system of equation per iteration.

5. Acknowledgements

The authors would like to acknowledge the financial support of Eletronorte S.A.

6. References

Zienkiewicz O. C. and Taylor R. L., 2000, “Finite Elements Method, volume 3”, Ed Butterworth Heinemann, England.

Codina R., Vazquez M., Zienkiewicz O.C., 1998, General algorithm for compressible and incompressible flow – part III. The semi-implicit form, International Journal for Num. Methods in Fluids 27 13-32.

Chorin A. J., 1968, Numerical solution of the Navier Stokes equations, Mathematics of Computational vol. 22, p. 745-762

Teman R., 1969, Sur l’approximation de la solution des équations de Navier-Stokes par la Méthode de pas fractionaires, Archives for Tational Mechanics and Analysis, vol. 32, p. 135-153.

Codina R., 2001, Pressure stability in fractional step finite element methods for incompressible flows, J. of Comp. Physics, vol 170, p. 112-140

Codina R., 2002, CBS versus GLS stabilization of the incompressible Navier-Stokes equations and the role of the time step stabilization parameter, Comm. In Num. Methods in Engineering, vol 18, p 99-112.

Akin, J. E.; 1994, “Finite Elements for Analysis and Design”, Academic Press Ltd., London.

Ghia, U., Ghia, K. N., Shin, C. T., 1982, “High-Re Solutions for Incompressible Flow using the Navier-Stokes Problem”, J. Comp. Physics, 48, 387-411.

Macedo Antonini Pupppin, 1995, “Aplicação de Métodos de Elementos Finitos Totalmente Estabilizados – GLS – À Simulação Numérica de Escoamentos Laminares e Turbulentos” Dissertação de Mestrado em Engenharia Mecânica Departamento de Engenharia Mecânica, Universidade de Brasília.

Morgan, K., Periaux, J., Thomasset, F., 1982, “Analysis of Laminar Flow over a Backward Facing Step”, A GAMM-Workshop, Friedr. Vieweg & Sohn.

Rhee H. S., Koseff J. R. e Street R. L., 1984, “Flow visualization of a recirculating flow by rheoscopic liquid and liquid crystal techniques”, Experiments in Fluids 2, 57-64.

7. Responsibility notice

The authors are the only responsible for the printed material included in this paper.